



Fermilab

TM-1118
1620.00

HYSTERESIS OF SEXTUPOLE AND AC LOSS
IN ENERGY DOUBLER DIPOLE MAGNETS

Kenji Ishibashi

June 18, 1982

A simple model was utilized for calculation of magnetization effects on ac loss and sextupole for Energy Doubler dipole magnets. The calculation in the simple model gave an underestimation of ac loss by about 30%. Results of computation on ac harmonics were also described.

1. INTRODUCTION

As is well known, superconducting magnets have inherently some hysteresis properties^{1,2} on magnetic field. This hysteresis comes mainly from magnetization of conductor. A study has been made by H. Ishimoto et al.³ on these magnetization effects for prototype Energy Doubler dipole magnets by use of conductor magnetization data taken experimentally, and a good agreement of those properties between computation and measurement was obtained. In the present report, nevertheless, a simple magnetization model⁴ was used for calculation because it is much easier to be done. An expression was derived for computation of magnetization effect on multipoles. It may be useful in a design of some other magnets to clarify the difference between experiment and calculation based on the simple model.

The ac loss of the Energy Doubler dipole magnets was decreased⁵ to a level of 500 joules for a regular current cycle by use of zebra conductors. Since the ac loss is so small and has a little ramp rate dependence around the regular ramp rate, ac harmonics are considered to be close to dc harmonics.

The hysteresis of sextupole was studied in dc harmonics, because the sextupole plays an important role in the accelerator, and most of its hysteresis comes from magnetization of the superconductor itself. The data of sextupole was utilized for estimation of critical current density of superconductor, and then to determine the relationship between hysteresis of sextupole and ac loss. The magnet numbers used in the present report ranged from No. 201 to 438.

2. EXPRESSION OF CONDUCTOR MAGNETIZATION EFFECTS

The magnetization of conductor may be written with a simple model⁴ by

$$-\vec{M} = M_0 \left[\vec{\beta} + \frac{1}{\lambda J_c d} \left\{ \frac{\dot{B} \vec{\beta} l^2}{\rho_e} + \frac{\dot{B}_L \vec{\beta}_L}{\rho_a} \left\{ \frac{4}{5} \alpha^2 + 1 \right\} + \frac{3}{4} \frac{\dot{B}_L \vec{\beta}_L L^2}{\alpha^2 \rho_a} \right\} \right] \quad (1)$$

$$M_0 = \frac{2k\mu_0\lambda J_c d}{3\pi} \quad (2)$$

where arrows stand for vectors, and $\vec{\beta}_L$, $\vec{\beta}_L$ and $\vec{\beta}$ show unit vectors expressing magnetic field direction. Eq. (2) shows magnetization of superconductor itself, and does not depend on ramp rate in this simple model.

If the permeability of iron is assumed to be infinite, a harmonic coefficient b_n due to the magnetization may be derived as follows for a single layer configuration shown in Figure 1.

$$B_0 b_n = \frac{n+1}{2\pi} \left[\int_{r_1}^{r_2} \frac{1 + \left(\frac{r}{R}\right)^{2(n+1)}}{r^{n+1}} \left\{ \int_0^{2\pi} M \cos \phi \cdot \sin(n+1)\theta d\theta \right\} dr \right. \\ \left. - \int_{r_1}^{r_2} \frac{1 - \left(\frac{r}{R}\right)^{2(n+1)}}{r^{n+1}} \left\{ \int_0^{2\pi} M \sin \phi \cdot \cos(n+1)\theta d\theta \right\} dr \right] \quad (3)$$

The derivation is described in the Appendix.

By use of the magnetization M , the ac loss Q may be computed by

$$Q = 2 \int \int M \frac{dB}{\mu_0} dv \quad (4)$$

Eqs. (1) and (2) are supposed to give some error in field below a few kG, due to partial flux penetration into superconducting filaments.

3. MEASUREMENT DATA OF HYSTERESIS OF SEXTUPOLE IN DC HARMONICS

The harmonics were measured at about 4.7K with a maximum 4000A at the Magnet Test Facility (MTF) with dividing the magnet bore tube into three sections; i.e., central section, upstream and downstream end sections. An off-center correction was made on the three data and then the corrected data was combined into the harmonics for a whole magnet.

Figure 2 shows examples of hysteresis of sextupole in the combined dc harmonics as a function of current. Square and circular marks stand for values at 660 and 2000A, respectively. The hysteresis of sextupole is almost constant for each current.

The hysteretic values of the sextupole were averaged for magnets No. 201 to 438. Figure 3 shows the difference between average hysteresis for the central section and combined data. The difference is divided by the combined data, and is plotted as a function of current. As seen from the Figure, the differences are small and at most 3%. This fact indicates that the end winding has a small anomalous effect on the hysteresis, and the Eq. (3) for the central section is applicable to a whole magnet. On the other hand, one can see from the Figure that the difference depends almost linearly on current, although a simple consideration suggests that the values should be constant.

Figure 4 shows average values of hysteresis of sextupole in the combined dc harmonics. The hysteresis of sextupole is multiplied by central field to obtain a suitable ordinate in the Figure. A current of 1 kA corresponds to a central field of 1T for the Energy Doubler dipole magnet. The hysteresis decreases with increasing current, because critical current density of superconductor; i.e., magnetization of superconductor decreases with increasing field in windings. Since the actual hysteresis of sextu-

pole is expressed by dividing the plotted data by central field B_0 , it has steeper dependence on current.

4. COMPARISON BETWEEN CALCULATION AND MEASUREMENT

Calculation was made by application of Eq. (3) to inner and outer layers of Energy Doubler dipole magnets. The only first term in Eq. (1) was utilized for giving the hysteresis of sextupole in dc harmonics. The unknown value was the critical current density J_c in Eq. (2). Table II shows the critical current density⁶ for fields of 5.0 to 6.0T at 4.7K. The short sample test was done at 4.3K, and the obtained current density was converted into the value at 4.7K by assuming the following relations.⁷

$$J_c = J_c(4.3) \cdot \frac{T_c^{-4.7}}{T_c^{-4.3}} \quad (5)$$

$$T_c = 9.0 \times (1 - 0.0456 \cdot B) \quad (6)$$

The critical current densities listed in the Table are the values averaged for 10 consecutive spools of conductor in the Fall of 1980.

For critical current densities for the other fields, Kim model was assumed.

$$J_c = J_0 \frac{B_2}{B+B_2} \quad (7)$$

The field B at each point in the winding was computed numerically by use of program POISSON. The parameters of J_0 and B_2 were chosen to give the experimental hysteresis of sextupole.

A solid line in Figure 4 shows the calculated results for the parameters of $J_0 = 2.08 \times 10^{10} \text{A/m}^2$ and $B_2 = 0.50 \text{T}$. The solid line is appreciably higher than the experimental values, but reproduces well the shape of it. A chain line in the Figure shows the results obtained by another parameter set, $J_0 = 1.76 \times 10^{10} \text{A/m}^2$ and $B_2 = 0.60 \text{T}$. As seen from the two lines, the calculated values of

hysteresis of sextupole around 3000A are quite insensitive to the set of J_0 and B_2 , while the calculated values below 1000A depend appreciably on the set of J_0 and B_2 . Then, the solid line is thought to be one of successful results with the assumption of Eq. (7).

The critical current density used for the solid line in the Figure is plotted by a solid line in Figure 5. Circular marks indicate the experimental values of critical current density. As far as the experimental data in Figure 4 are concerned, the critical current density in a region of roughly 0.5 to 4T in Figure 5 is considered to be higher than the actual current density.

Another assumption was then tried for the critical current density, and the following practical equation was taken for comparison with the solid line.

$$J_c = J_0 \cdot \exp\left(-\frac{B}{B_2}\right) + c \quad (8)$$

where J_0 , B_2 and c are adjustable parameters. This equation is useful empirically for superconductors which underwent heavy cold work.⁸

A dashed line in Figure 4 shows the calculated results with values of $J_0 = 1.45 \times 10^{10} \text{A/m}^2$, $B_2 = 0.60 \text{T}$ and $c = 0.174 \times 10^{10} \text{A/m}^2$. The dashed line agrees well with the experiment. A dashed line in Figure 5 indicates the current density used for this calculation. The critical current density is appreciably lower in the low field region than the solid line. Nevertheless, the experimental data in Figure 5 suggests that the solid line may be more plausible than the dashed line, because the solid line seems to agree better with the experimental values at 5.0 to 6.0T than the dashed line.

5. RELATION BETWEEN HYSTERESIS OF SEXTUPOLE AND AC LOSS

The experimental hysteresis of sextupole is plotted in Figure 6 as a function of experimental ac loss. Square and circular marks stand for experimental values at currents of 660 and 2000A, respectively. The abscissa shows values of ac loss at a zero ramp

rate which were extrapolated from the experimental data of ramp rate dependence of ac loss with a maximum current of 2000A.

The plotted points for each current are concentrated in a certain zone, except a few data. The ac loss data is scattered in a rather wide region, particularly seen at 2000A. This may be because there was a ground loop current effect in the integrator used for the measurement. If a correction was made for the ground loop current effect, it would make the data be concentrated in a smaller zone. The loop effect was decreased later at MTF.

A calculation was made for ac loss by use of Eq. (4). The only first term in Eq. (1) was considered, and the field in the winding was obtained by the program POISSON again. Triangular marks in Figure 6 indicate the calculated values for critical current density which is shown by the solid line in Figure 5. Cross marks corresponding to the dashed line in Figure 5 are given for comparison. One can see from the Figure that the difference of ac loss between calculation and experiment is about 60 joules for the triangular marks, and about 100 joules for cross.

For the difference between experiment and calculation in the Figure, the following reasons are considered. The first is an effect from the simple model in calculation. In fact, Eq. (2) is known to give an underestimation of ac loss by 10 to 20%, probably due to neglectation of some coupling currents through filaments. These coupling effects are thought to be different from the coupling which is written in the second term in Eq. (1), and to appear even in a quite slow ramp rate. Since twisting is indeed not a transposition, this may be the coupling between the concentric layers of filaments.⁸ The values of ac loss were extrapolated from the data of ramp rate dependence, and those values may still contain the effect from the coupling mentioned above.

The second comes about from other metallic parts of the magnet. There are three stainless steel tubes inside the coil during measurement at MTF. Outside the coil are the collars and five concentric stainless steel tubes for cryostat. However, the ramp

rate concerned is so slow (~2kG/s) that the eddy current effects are very small^{5,9} on ac loss. Some contribution from the metallic parts may be made by a laminated iron yoke. Since the iron is apart from the coil, the hysteresis of iron magnetization have a small effect on ac loss and sextupole, and it contributes several percent to the total hysteresis of sextupole.³

6. ESTIMATION OF AC HARMONICS

By use of Eq. (1), a calculation of ac harmonics was made for a ramp rate of 225A/s. The effective resistivity across single strand ρ_e was taken¹⁰ in Eq. (1) as $4.1 \times 10^{-10} \Omega\text{m}$. The average transverse resistivity across cable ρ_a was simply estimated from measurement of M.Kuchnir⁶ which is shown in Figure 7. A certain section of actual magnet winding made of Ebonal conductor was cut out, and resistivity between two arbitrary strands was measured at a temperature of 4.3K. The ordinate stands for resistance for unit length, and the abscissa for number of contact lines between two strands. If two adjacent strands are chosen, the number of contact lines is unity. The resistance for unit length ranges from 17 to $35 \mu\Omega \cdot \text{m}$. The resistance increases with the number of contact lines, and is saturated at a number of 5. The saturation is due to direct crossed contacts of strands. The low resistance for numbers below 5 comes about mainly from current flowing strands paralleled between the two strands.

Because there are two crossed contacts in a length of transposition pitch for any combination of two strands, the resistance for each crossed contact is written for the data for numbers above 5 by

$$R_c = 2 \frac{1}{4L} R_m \quad (9)$$

The average transverse resistivity ρ_a is therefore expressed by

$$\rho_a = R_c \cdot 2a \left(\frac{W}{L} + \frac{L}{W} \right) \quad (10)$$

When Eqs. (9) and (10) are applied to experimental results for numbers below 5, the value of ρ_a is given to be 1.4 to $4.6 \times 10^{-7} \Omega\text{m}$ for experimental resistivities of 17 to $53 \mu\Omega \cdot \text{m}$. For the zebra

conductors, the value of ρ_a is considered to be a little lower than that of Ebonal conductors, and it is probably a value around or below $10^{-7}\Omega\text{m}$.

The calculated results on sextupole of ac harmonics at 2000A at a ramp rate of 225A/s are shown in Figure 8. The sextupole of dc harmonics is subtracted from that of ac harmonics, and it is plotted as a function of ρ_a after being multiplied by central field B_0 . In the Figure, the difference is -0.48 G/in^2 at $\rho_a = 4.6 \times 10^{-7}\Omega\text{m}$, and this means the sextupole of ac harmonics is $0.24 \times 10^{-4} \text{ in}^{-2}$ lower at 2000A than that of dc harmonics. As the experimental magnetization effect on hysteresis of sextupole in dc harmonics is $1.8 \times 10^{-4} \text{ in}^{-2}$ at 2000A in Figure 4, the value of $0.24 \times 10^{-4} \text{ in}^{-2}$ is fairly lower than that. One can see in Figure 8 that the difference is saturated to -0.47 G/in^2 around $\rho_a = 10^{-6}\Omega\text{m}$. This value corresponds to the second term in Eq. (1), and shows the effect from the coupling current through twisted filaments.

7. CONCLUSION

A study of hysteresis of sextupole and ac loss was made with assumption of the simple model. The results obtained are as follows:

- a. The calculation in assumption of the simple model gave an underestimation of ac loss by about 30%, and gave an overestimation of hysteresis of sextupole, for example, by $0.4 \times 10^{-4} \text{ in}^{-2}$ at 3000A.
- b. It was shown by calculation that a ramp rate of 225 A/s has a small effect on sextupole.

ACKNOWLEDGEMENTS

The author wishes to acknowledge Dr. A.D.McInturff for his useful suggestions.

REFERENCES

1. R.Yamada, H.Ishimoto and M.E.Price, IEEE Trans. Magn. MAG-13, 56 (1977).
2. A.D.McInturff and D.A.Gross, IEEE Trans. Nucl. Sci. NS-28, No. 3, 3211 (1981).
3. H.Ishimoto, R.E.Peters, M.E.Price and R.Yamada, IEEE Trans. Nucl. Sci. NS-24, No. 3, 1303 (1977).
4. M.N.Wilson, Rutherford Laboratory Report RHEL/M/A26 (1972).
5. M.Wake, D.A.Gross, R.Yamada and D.Blatchley, IEEE Trans. Magn. MAG-15, No. 1, 141 (1979).
6. M.Kuchnir, private communication.
7. K.Ishibashi, M.Wake, M.Kobayashi and A.Katase, Cryogenics, 19, 67 (1979).
8. A.D.McInturff, private communication.
9. R.E.Shafer, IEEE Trans. Magn. MAG-17, No. 1, 722 (1981).
10. H.Ishimoto, R.Yamada and R.E.Pighetti, Fermilab Report TM-636 (1975).

APPENDIX

Since complex functions are useful for two dimensional calculation, they are employed in this Appendix. By use of complex function, the magnetization vector M can be written as $Me^{i\theta}$, where $e^{i\theta}$ shows the direction of the magnetization. For the magnetization $Me^{i\theta}$ of conductors shown in Figure 1, the induced field B_m at location z can be expressed as

$$B_m^* = \frac{1}{2\pi} \int \left\{ \frac{Me^{i\theta}}{(z-z_0)^2} + \frac{R^2}{z_0^{*2}} \cdot \frac{Me^{-i\theta}}{\left(z - \frac{R^2}{z_0^*}\right)^2} \right\} dv \quad (A-1)$$

where $z_0 = re^{i\theta}$ and $dv = r dr d\theta$. The second term in the integral stands for mirror effect from the surrounding iron. Because $|z| < |z_0| < \frac{R}{|z_0^*|}$ the Taylor expansion leads to the following:

$$\frac{1}{(z-z_0)^2} = \sum_{n=0}^{\infty} \frac{n+1}{z_0^{n+2}} z^n \quad (A-2)$$

$$\frac{1}{\left(z - \frac{R^2}{z_0^*}\right)^2} = \sum_{n=0}^{\infty} \frac{(n+1) z_0^{*(n+2)}}{R^{2(n+2)}} z^n \quad (A-3)$$

Putting Eqs. (A-2) and (A-3) to (A-1), the field is written by

$$B_m^* = \sum_{n=0}^{\infty} C_n \cdot z^n \quad (A-4)$$

$$C_n = \frac{n+1}{\pi} \iint \frac{1}{r^{n+1} e^{i(n+1)\theta}} \left\{ Me^{i\theta} + \left(\frac{r}{R}\right)^{2(n+1)} Me^{-i\theta} \right\} dr d\theta \quad (A-5)$$

where $\phi = \theta - \theta$.

The imaginary part of Eq. (A-5) gives Eq. (3) in the text.

TABLE INOTATION

\vec{M}	: Magnetization vector
M	: Magnetization
M_0	: Intrinsic magnetization of cable
$\vec{\beta}$: Unit vector in a magnetic field direction
$\vec{\beta}_\perp$: Unit vector in a direction perpendicular to cable
$\vec{\beta}_\parallel$: Unit vector in a direction parallel to cable
λ	: Superconductor fraction of single strand
J_C	: Critical current of superconductor
d	: filament diameter
B	: Magnetic field
\dot{B}	: Field changing rate
\dot{B}_\perp	: Field changing rate in a direction perpendicular to cable
\dot{B}_\parallel	: Field changing rate in a direction parallel to cable
$4l$: Twist length of single strand
$4L$: Transposition length of cable
ρ_e	: Effective transverse resistivity across single strand
ρ_a	: Average transverse resistivity across cable
α	: Aspect ratio of cable
k	: Compaction density of cable
μ_0	: Permeability of vacuum
B_0	: Central field of dipole magnet
b_n	: Normal multipole coefficient of n'th order
r_1	: Inner radius of coil
r_2	: Outer radius of coil
R	: Inner radius of iron
ϕ	: Angle between \vec{r} and \vec{M}
Q	: ac loss
v	: Volume
T_C	: Transition temperature of superconductor
J_0	: Critical current density of zero field in Kim model
B_2	: Field parameter for critical current density
c	: Adjustable parameter for critical current density
R_C	: Resistance for crossed contact
R_m	: Resistance for a unit length of cable
$2a$: Thickness of cable
$2w$: Width of cable

TABLE IICRITICAL CURRENT DENSITY

Data at 4.7K was extrapolated from the measurement at 4.3K.

Field	<u>Temperature</u>	
	4.3K	4.7K
6.0T	$1.86 \times 10^9 \text{A/m}^2$	$1.53 \times 10^9 \text{A/m}^2$
5.5T	2.07	1.74
5.0T	>2.27	>1.93

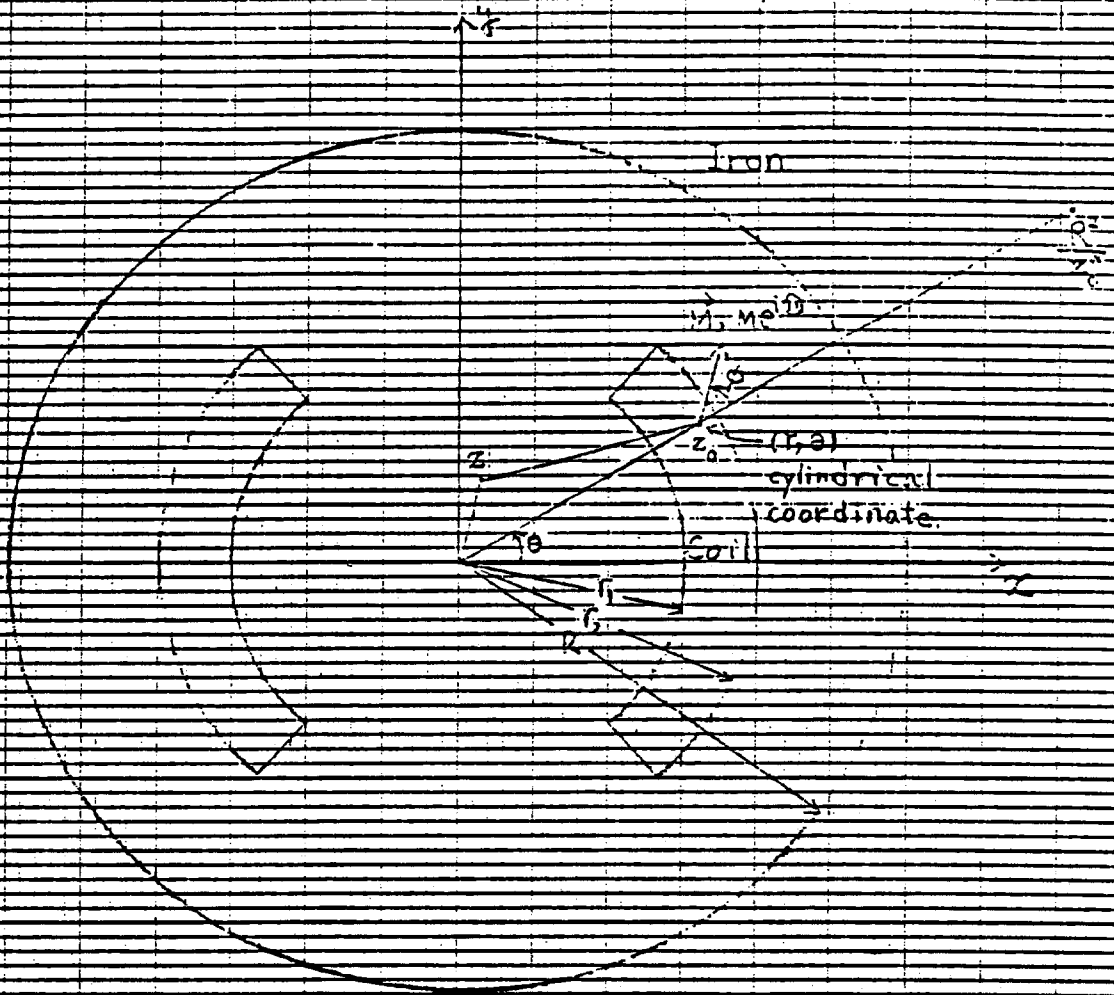


Fig. 1 Coordinate system for calculation of harmonics due to conductor magnetization

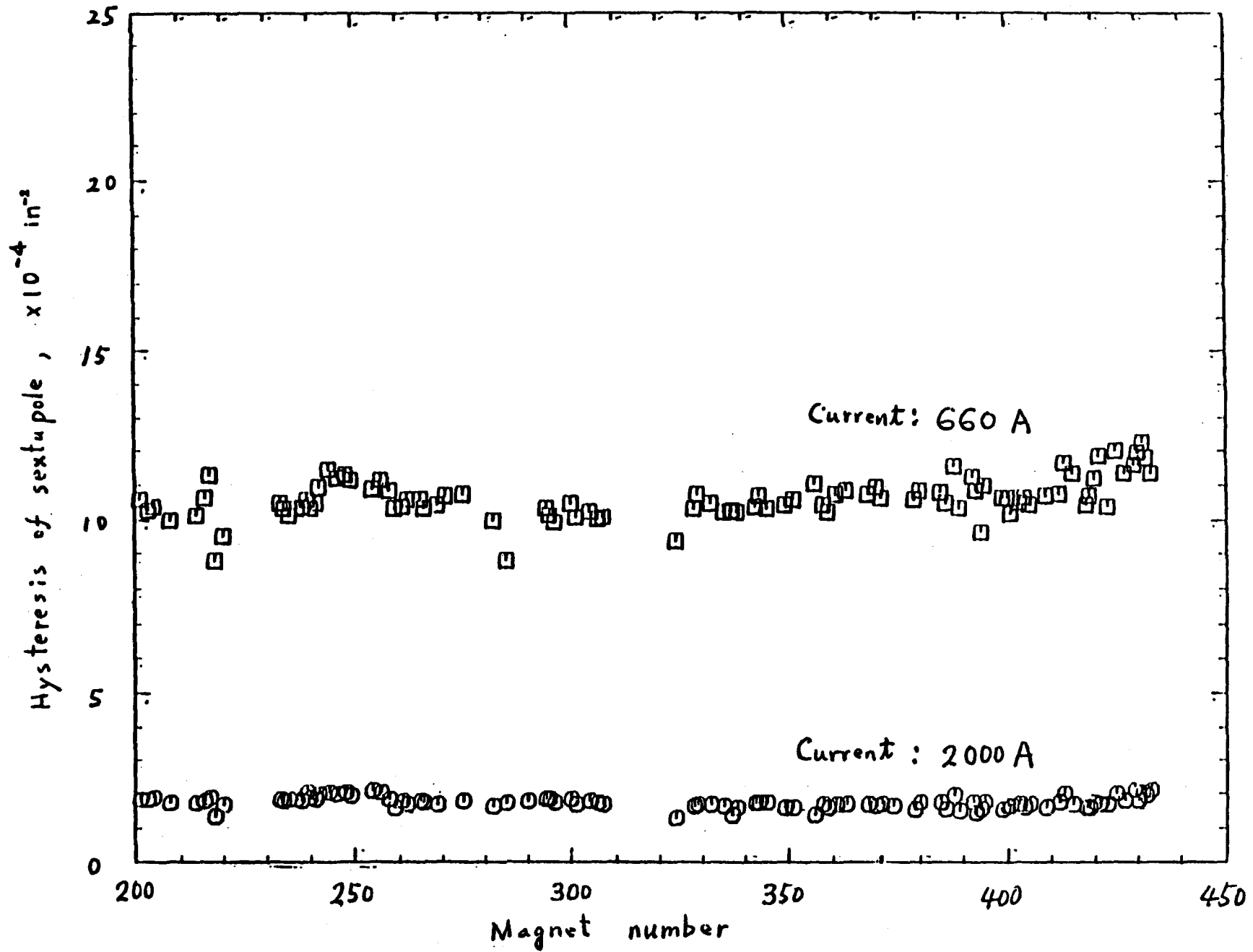


Fig. 2 Hysteresis of sextupole vs. magnet number

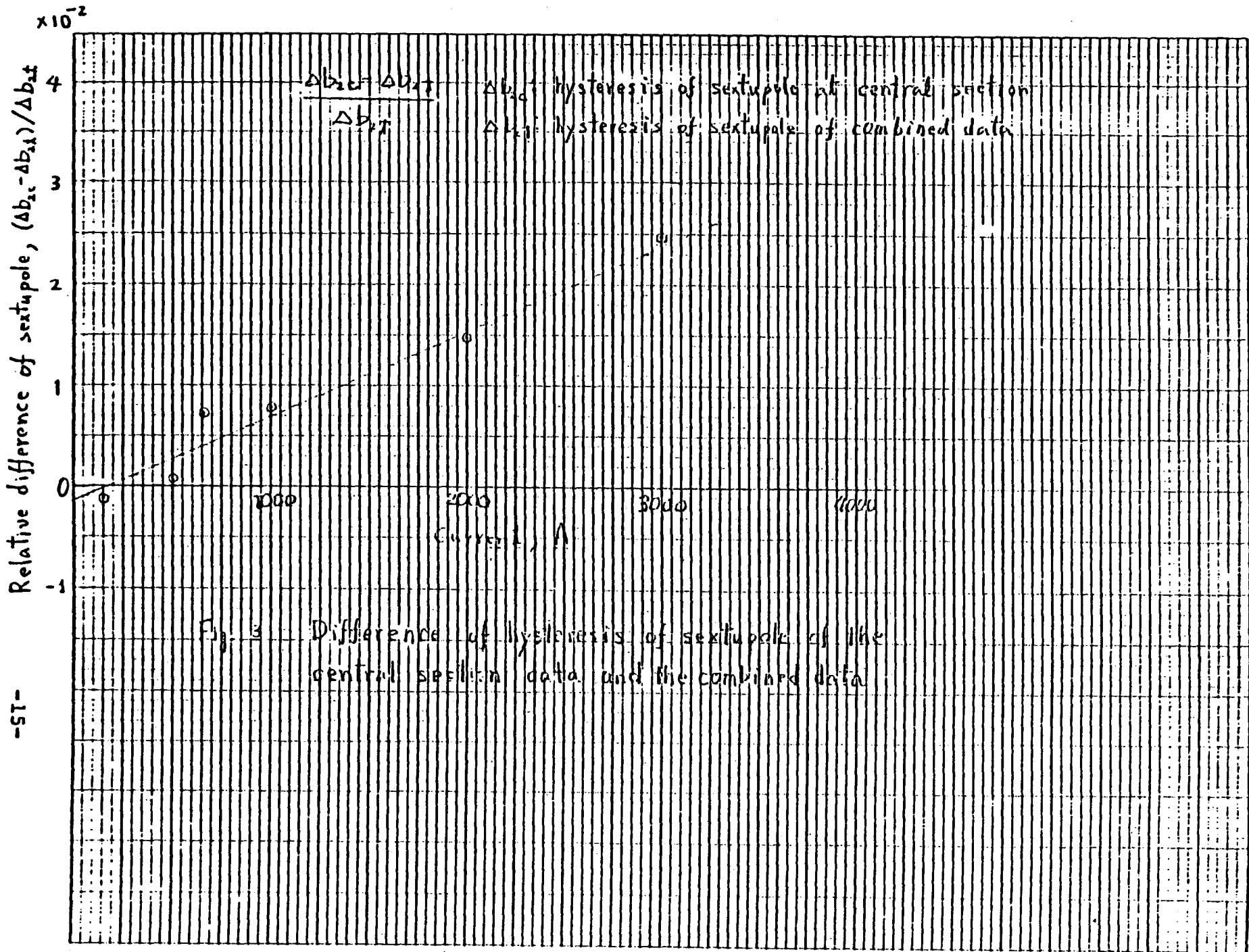
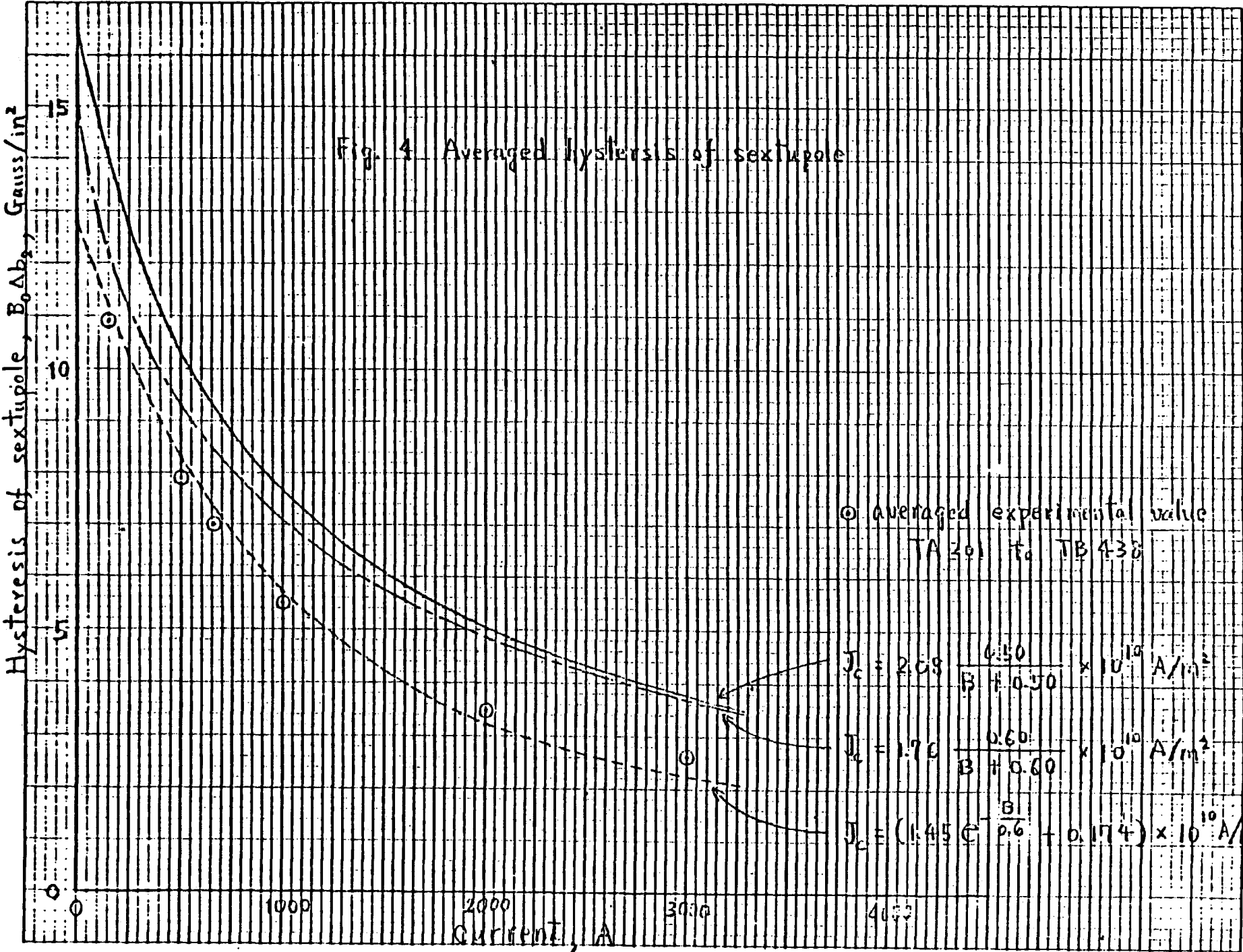
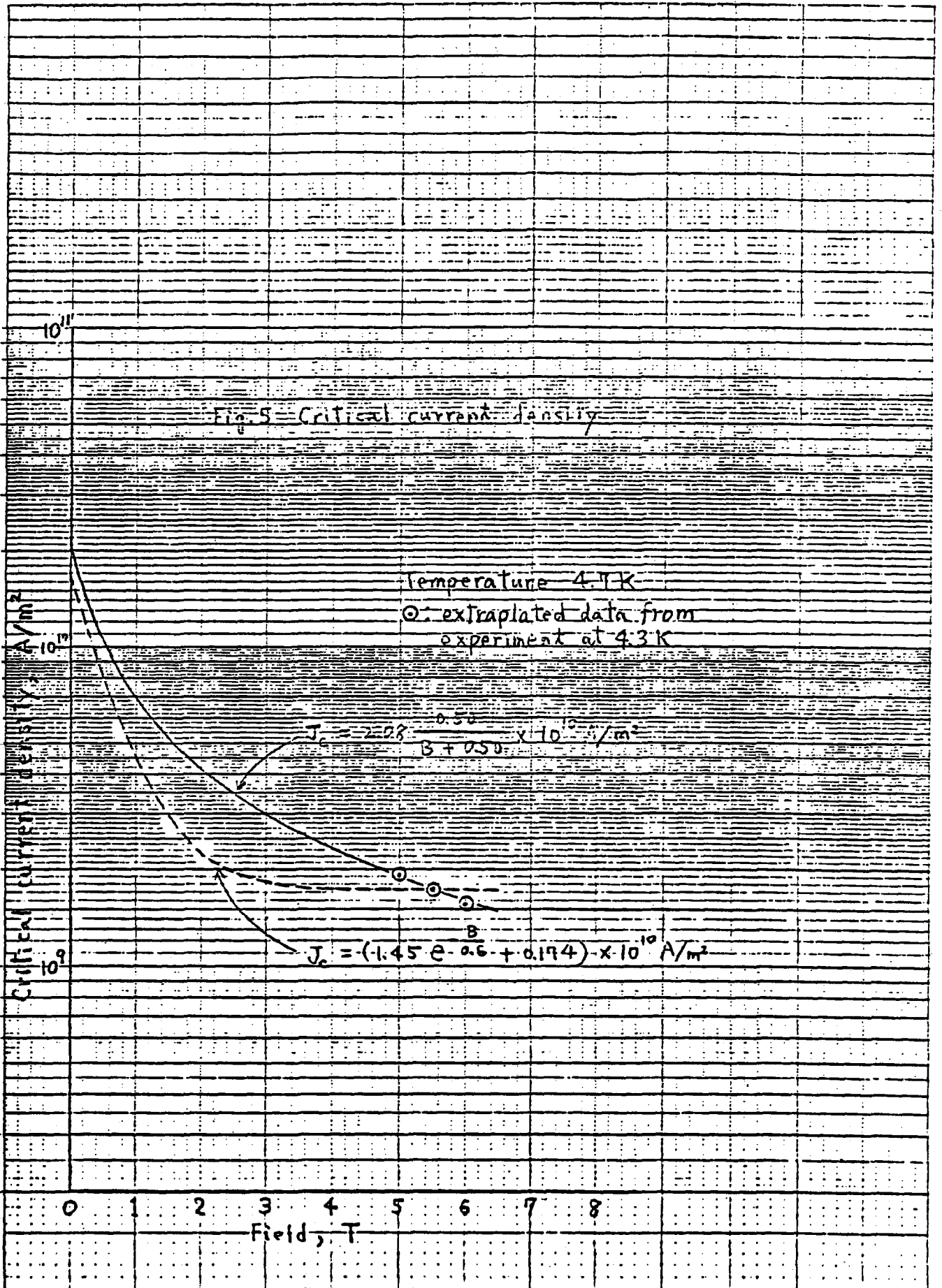


Fig. 3 Difference of hysteresis of sextupole of the central section data and the combined data





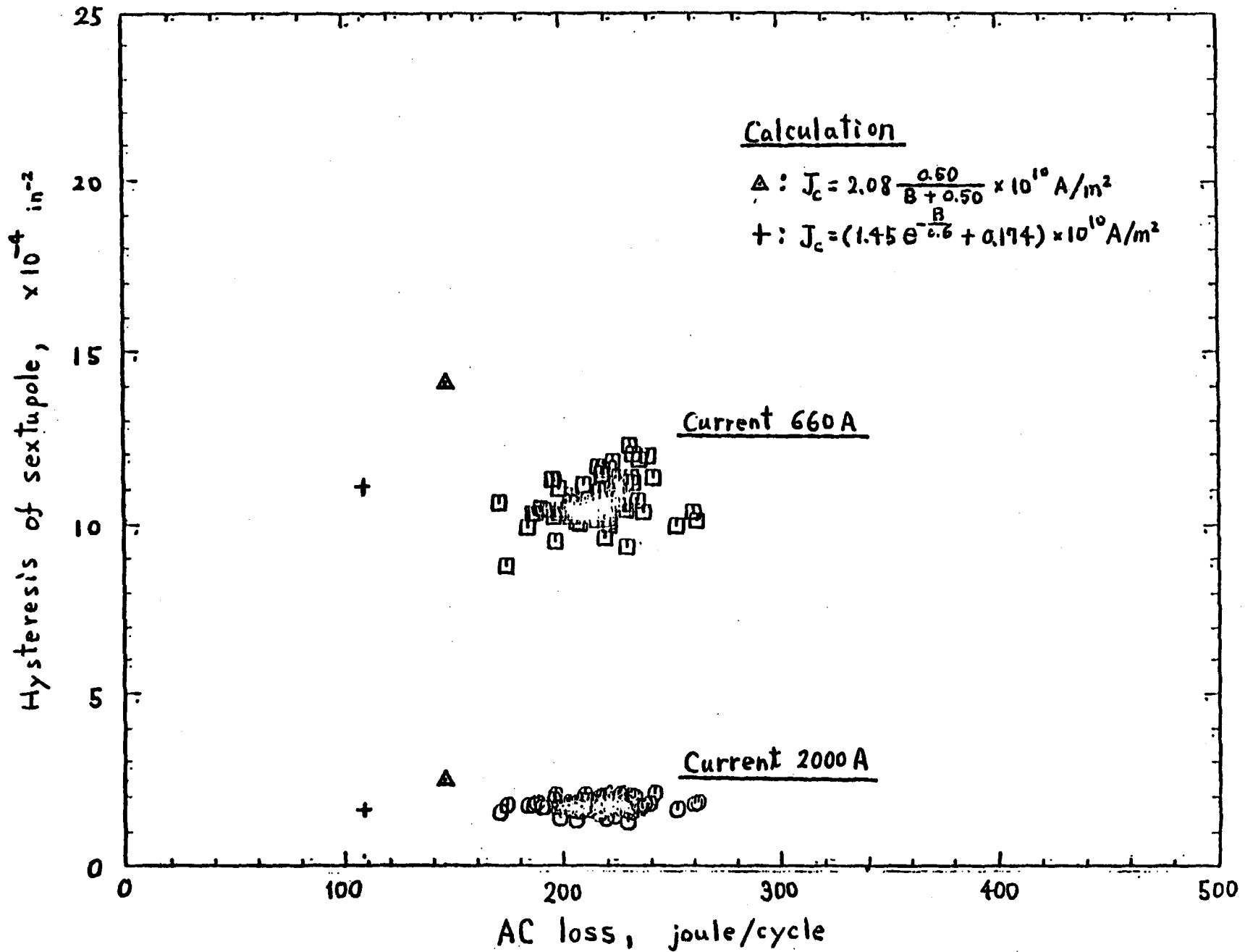


Fig. 6 Relationship between hysteresis of sextupole and AC loss

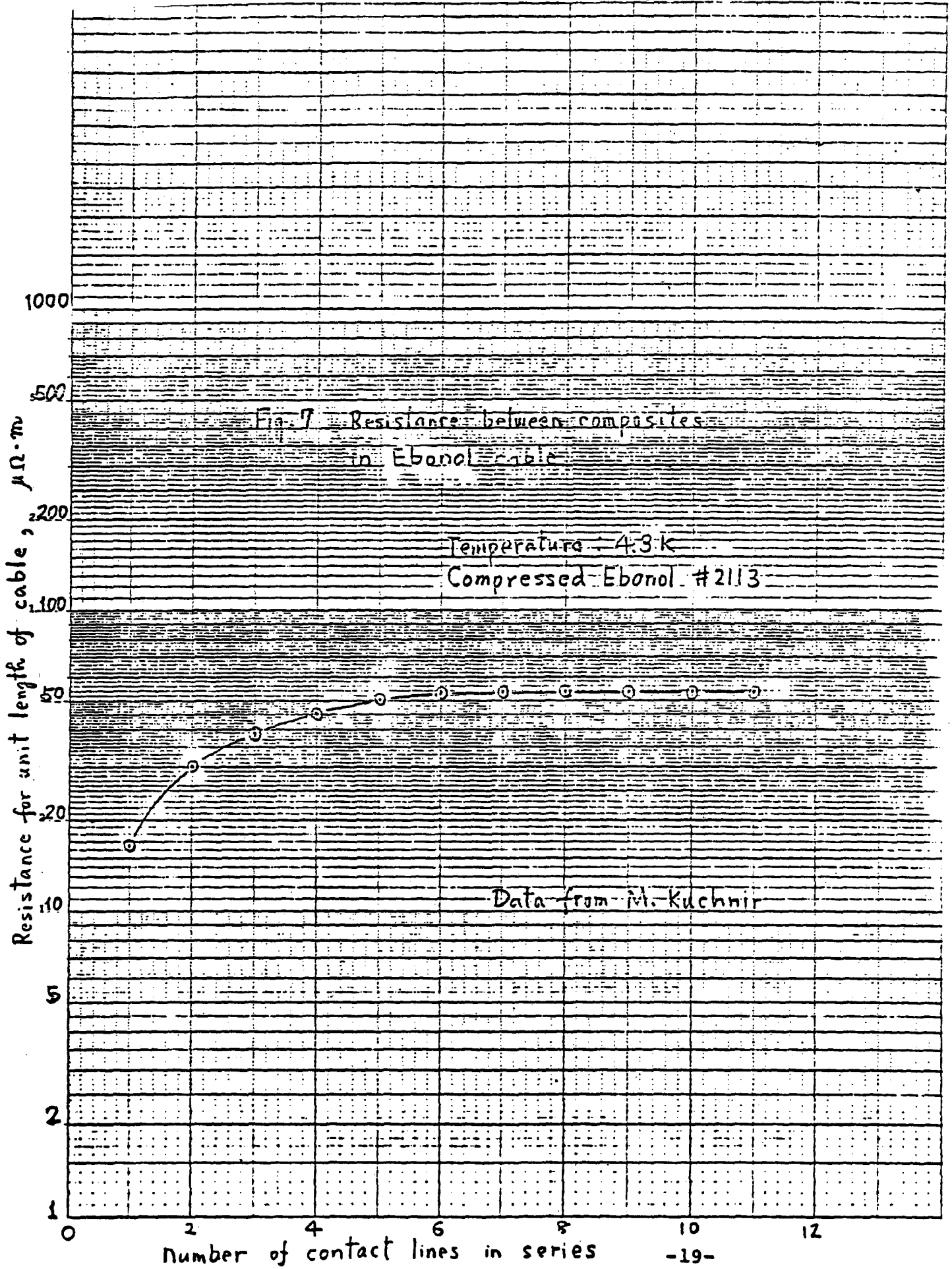


Fig. 8 Difference between AC and DC
harmonics

Effective transverse resistivity
across single strand

$$\rho_e = 4.3 \times 10^{-9} \Omega \cdot \text{m}$$

Ramp rate = 225 A/s

Current = 2000 A

